anomaly, morphotropic phases need to be determined under high electric-field driving. However, this evaluation is very difficult to perform, and is left for future studies.

On the other hand, it is obvious in Fig. 4a that the textured LF4T, which is the ⟨001⟩ orientated ceramic, exhibited a large strain nearly double of that of the non-textured LF4 ceramic, and the strain was even larger than the field-induced strain for PZT4. In addition, we discovered that the texture given to LF4 not only enhanced the field-induced strain but also improved the temperature coefficient of normalized strain (S_{max}/E_{max}), as shown in Fig. 4a, where S_{max} and E_{max} denote the maximum strain and the maximum electric field strength, respectively. That is to say, the texture stabilizes the temperature-dependent strain characteristic of LF4T, even though its transformation temperature between orthorhombic and tetragonal phases is the same as that of non-textured LF4 in the unpoled state. Furthermore, it should be noted that the flat, temperature-independent characteristic of LF4T is even more prominent than PZT4, since the strain deviation value of 6.5% for LF4T between room temperature and 160 °C is smaller than that of 15% for PZT4. This piezoelectric strain behaviour of LF4T is of great importance for temperature-independent actuator devices.

The temperature-independent strain characteristics (for a given texture) are the result of changes in the amplitude of, and in the ratio between, two strain components; one from a lattice motion and the other from domain wall motion[28–30]. Those two field-induced strain components must be dependent on temperature and microstructure (that is, textured or non-textured). In order to clarify the underlying mechanism, a measurement system needs to be developed for the separate evaluation of strain components from the two different origins.

The overall performance of the developed LF4T ceramic is listed in Fig. 4b with that of the typical high-performance PZT ceramic (PZT4). It is clear that most of the piezoelectric properties are comparable to those of the PZT. This high performance leads us to expect that the developed materials are leading candidates for environmentally friendly piezoelectric devices. □

Methods

$Bi_{2.5}Na_{3.5}Nb_5O_{18}$ (BiNN5) platelet was synthesized at 1,100 °C using molten NaCl salt as a flux. Using a topochemical reaction, $NaNbO_3$ platelet was synthesized from BiNN5 and a complementary reactant, Na_2CO_3, in a NaCl flux at 950 °C, and Bi_2O_3, the by-product, was removed. The synthesized $NaNbO_3$ had the same morphology as BiNN5, 0.5 μm in thickness and 10–15 μm in side length of a developed area, and consisted of a single-phase perovskite with no secondary phase detected by XRD. The $NaNbO_3$ platelets (as reactive templates) and complementary reactants—equiaxed $NaNbO_3$, $KNbO_3$, $KTaO_3$, $LiSbO_3$ and $NaSbO_3$ particles—were mixed, tape-cast and stacked. The textured $(K_{0.44}Na_{0.52}Li_{0.04})(Nb_{0.84}Ta_{0.10}Sb_{0.06})O_3$ polycrystal (LF4T) was prepared by sintering the stacked tape at 1,135 °C.

The piezoelectric d_{31} constants were measured by the resonance anti-resonance method with an impedance analyser (Agilent, HP4194A). The piezoelectric d_{33} constants were measured by the direct piezoelectric method using a piezo-d_{33} meter (Institute of Acoustic Academia Sinica, model ZJ-4B). The degree of tetragonal ⟨001⟩ axis orientation, F, was evaluated by the Lotgering's equation using an X-ray diffractometer (Rigaku, RINT TTR2, CuKα radiation).

Received 25 May; accepted 3 September 2004; doi:10.1038/nature03028.
Published online 31 October 2004.

1. Haertling, G. E. Ferroelectric ceramics: History and technology. *J. Am. Ceram. Soc.* **82,** 797–818 (1999).
2. Takenaka, T. & Nagata, H. Present status of non-lead-based piezoelectric ceramics. *Key Eng. Mater.* **157–158,** 57–64 (1999).
3. Jaeger, R. E. & Egerton, L. Hot pressing of potassium-sodium niobates. *J. Am. Ceram. Soc.* **45,** 209–213 (1962).
4. Dungan, R. H. & Golding, R. D. Polarization of $NaNbO_3$-$KNbO_3$ ceramic solid solutions. *J. Am. Ceram. Soc.* **48,** 601 (1965).
5. Haertling, G. H. Properties of hot-pressed ferroelectric alkali niobate ceramics. *J. Am. Ceram. Soc.* **50,** 329–330 (1967).
6. Egerton, L. & Bieling, C. A. Isostatically hot-pressed sodium-potassium niobate transducer material for ultrasonic devices. *Ceram. Bull.* **47,** 1151–1156 (1968).
7. Aurivillius, B. Mixed bismuth oxides with layer lattices. *Ark. Kemi* **1,** 499 (1949).
8. Wood, A. Polymorphism in potassium niobate, sodium niobate, and other ABO_3 compounds. *Acta Crystallogr.* **4,** 353–362 (1951).
9. Buhrer, C. F. Some properties of bismuth perovskites. *J. Chem. Phys.* **36,** 798–803 (1962).
10. Nitta, T. Properties of sodium-lithium niobate solid solution ceramics with small lithium concentrations. *J. Am. Ceram. Soc.* **51,** 626–629 (1968).
11. Scot, B. A., Giess, E. A., Burns, G. & O'Kane, D. F. Alkali-rare earth niobates with the tungsten bronze-type structure. *Mater. Res. Bull.* **3,** 831–842 (1968).
12. Hellwege, K.-H., Hellwege, A. M., Mitsui, T. & Nomura, S. (eds) *Numerical Data and Functional Relationships in Science and Technology*, New Series Group 3: *Crystal and Solid State Physics*, Vol. 16, *Ferroelectrics and Related Substances* Subvol. a, *Oxides* (Springer, Berlin, 1981).
13. Mitsui, T. & Nakamura, E. (eds) *Numerical Data and Functional Relationships in Science and Technology*, New Series Group 3: *Crystal and Solid State Physics*, Vol. 28, Suppl. and Extension to Vol. 16, *Ferroelectrics and Related Substances* Subvol. a, *Oxides* (Springer, Berlin, 1990).
14. Takenaka, T. & Nagata, H. *Program Summary and Extended Abstract of the 11th US-Japan Seminar on Dielectric and Piezoelectric Ceramics* 237–244 (US-Japan seminar committee, Sapporo, Hokkaido, Japan, 2003).
15. Jaffe, B., Roth, R. S. & Marzullo, S. Properties of piezoelectric ceramics in the solid-solution series lead titanate zirconate-lead oxide: tin oxide and lead titanate-lead hafnate. *J. Res. Natl Bur. Stand.* **55,** 239–254 (1955).
16. Zhang, S. J., Randall, C. A. & Shrout, T. R. High Curie temperature piezocrystals in the $BiScO_3$-$PbTiO_3$ perovskite system. *Appl. Phys. Lett.* **83,** 3150–3152 (2003).
17. Jaffe, B., Cook, W. R. & Jaffe, H. *Piezoelectric Ceramics* (Academic, New York, 1971).
18. Cohen, R. E. Origin of ferroelectricity in perovskite oxides. *Nature* **358,** 136–138 (1992).
19. Lotgering, F. K. Topotactical reactions with ferrimagnetic oxides having hexagonal crystal structures — I. *J. Inorg. Nucl. Chem.* **9,** 113–123 (1959).
20. Takenaka, T. & Sakata, K. Grain orientation and electrical properties of hot-forged $Bi_4Ti_3O_{12}$ ceramics. *Jpn. J. Appl. Phys.* **19,** 31–39 (1980).
21. Kimura, T., Yoshimoto, T., Iida, N., Fujita, Y. & Yamaguchi, T. Mechanism of grain orientation during hot-pressing of bismuth titanate. *J. Am. Ceram. Soc.* **72,** 85–89 (1989).
22. Watanabe, H., Kimura, T. & Yamaguchi, T. Sintering of platelike bismuth titanate powder compacts with preferred orientation. *J. Am. Ceram. Soc.* **74,** 139–147 (1991).
23. Brahmaroutu, B., Messing, G. L., Trolier-Mckinstry, S. & Selvaraj, U. in *Proc. 10th IEEE Int. Symp. on Applications of Ferroelectrics* Vol. 2 (eds Kulwicki, B., Amin, A. & Safari, A.) 883–886 (Institute of Electrical and Electronic Engineers (IEEE), Piscataway, NJ, 1996).
24. Horn, J. A., Zhang, S. C., Selvaraj, U., Messing, G. L. & Trolier-McKinstry, S. Templated grain growth of textured bismuth titanate. *J. Am. Ceram. Soc.* **82,** 921–926 (1999).
25. Tani, T. Crystalline-oriented bulk ceramics with a perovskite-type structure. *J. Korean Phys. Soc.* **32** (Suppl. Iss.), S1217–S1220 (1998).
26. Takeuchi, T., Tani, T. & Saito, Y. Piezoelectric properties of bismuth layer-structured ferroelectric ceramics with a preferred orientation processed by the reactive templated grain growth method. *Jpn. J. Appl. Phys.* **38,** 5553–5556 (1999).
27. Sugawara, T., Shimizu, M., Kimura, T., Takatori, K. & Tani, T. Fabrication of grain oriented barium titanate. *Ceram. Trans.* **136,** 389–406 (2003).
28. Saito, Y. Measurement of complex piezoelectric d_{33} constant in ferroelectric ceramics under high electric field driving. *Jpn. J. Appl. Phys.* **34,** 5313–5319 (1995).
29. Saito, Y. Measurement system for electric field-induced strain by use of displacement magnification technique. *Jpn. J. Appl. Phys.* **35,** 5168–5173 (1996).
30. Saito, Y. Hysteresis curve of X-ray diffraction peak intensity in lead zirconate titanate ceramics. *Jpn. J. Appl. Phys.* **36,** 5963–5969 (1997).

Acknowledgements We thank T. Takeuchi for technical contributions to the development of the processing; T. Saito for discussions; and N. Watanabe, M. Uoshima, H. Morisaka, Y. Aoki, K. Horibuchi, K. Hisazato, M. Okumura, M. Okano, K. Nomura and S. Tsuru for technical assistance.

Competing interests statement The authors declare competing financial interests: details accompany the paper on Nature's website (**http://www.nature.com/nature**).

Correspondence and requests for materials should be addressed to Y.S. (ysaito@mosk.tytlabs.co.jp).

Fire-induced erosion and millennial-scale climate change in northern ponderosa pine forests

Jennifer L. Pierce[1], **Grant A. Meyer**[1] **& A. J. Timothy Jull**[2]

[1]*Department of Earth and Planetary Science, University of New Mexico, Albuquerque, New Mexico 87131, USA*
[2]*NSF-Arizona AMS Facility, The University of Arizona, Tucson, Arizona 85721, USA*

Western US ponderosa pine forests have recently suffered extensive stand-replacing fires followed by hillslope erosion and sedimentation[1–4]. These fires are usually attributed to increased stand density as a result of fire suppression, grazing and other land use, and are often considered uncharacteristic or

unprecedented[1–3]. Tree-ring records from the past 500 years indicate that before Euro-American settlement, frequent, low-severity fires maintained open stands[1–3]. However, the pre-settlement period between about AD 1500 and AD 1900 was also generally colder than present[5–10], raising the possibility that rapid twentieth-century warming promoted recent catastrophic fires. Here we date fire-related sediment deposits in alluvial fans in central Idaho to reconstruct Holocene fire history in xeric ponderosa pine forests and examine links to climate. We find that colder periods experienced frequent low-severity fires, probably fuelled by increased understory growth. Warmer periods experienced severe droughts, stand-replacing fires and large debris-flow events that comprise a large component of long-term erosion[11] and coincide with similar events in sub-alpine forests of Yellowstone National Park[12]. Our results suggest that given the powerful influence of climate, restoration of processes typical of pre-settlement times may be difficult in a warmer future that promotes severe fires.

Fire regimes in western US conifer forests vary spatially with local climate[2,13,14]. Cool, moist, high-elevation spruce-fir forests experience severe, infrequent stand-replacing crown fires, whereas frequent light surface fires are considered typical of warm, xeric ponderosa pine (*Pinus ponderosa*) forests[1–3,13]. Over the twentieth century, fire size and severity have increased in most ponderosa pine forests, including those in the northern Rocky Mountains. From 1908 to 2000, canopy fires burned 50% of the Boise National Forest in central Idaho, mostly during severe droughts in 1926–35 and 1986–2000. Recent stand-replacing fires in this area have led to numerous large debris flows and sediment-charged floods in steep mountain drainages[4]. Sediment yields from single large sedimentation events following severe 1989 and 1994 fires[4] are three orders of magnitude greater than annual sediment yields measured without large events[11].

To assess the role of longer-term climatic variations on fire and erosion in northern ponderosa pine forests, we date fire-related deposits in tributary alluvial fans of the South Fork Payette River area, central Idaho (SFP; Fig. 1). These fans receive sediment from small (0.01–6 km^2), steep basins in weathered Idaho batholith granitic rocks, where post-fire erosion is likely. Annual precipitation is ~600–1,000 mm, with a marked summer drought conducive to fires. Ponderosa pines are common at lower elevations (~850–1,300 m) and on dry south-facing slopes. Mixed Douglas-fir (*Pseudotsuga menziesii*) and ponderosa pine stands dominate mid-elevation (~1,500–1,800 m) and north-facing slopes, and mixed conifers dominated by Douglas-fir and Engelmann spruce (*Picea engelmannii*) characterize high elevations around 2,000 m.

Post-fire debris-flow events and sediment-charged floods are produced via two primary mechanisms in the SFP area[4]. (1) After severe burns, reduced infiltration and smooth soil surfaces greatly increase surface runoff, typically during moderate- to high-intensity convective storms[15]. Extreme discharges entrain sediment through slope wash, rilling and gullying[4,12]. In lower-severity burns, discontinuous runoff generation limits sediment yields from post-fire storm events[16]. (2) Loss of root strength a few years after tree mortality promotes shallow landslides[17], usually during major winter storms. Storms that strike severe burns often produce thick, bouldery, charcoal-rich debris-flow deposits, but large debris flows may exist as only thin marginal facies at some alluvial fan sites[4,12]. Discrete layers of charred forest litter provide another stratigraphic indicator of fire. These well-preserved burned soil surfaces imply rapid burial by post-fire sediments before bioturbation. We define large fire-related events ('large events') conservatively as debris-flow units with abundant coarse angular charcoal (Supplementary Fig. 1) that are coarser grained than other units in a stratigraphic section, and comprise at least 20% of its thickness; most overlie burned soil surfaces. Deposits that do not meet these criteria but that contain abundant charcoal and (or) overlie burned surfaces are considered small fire-related events ('small events'). Multiple events that occurred hours to several years after a single fire may appear as a single thick deposit that would be recognized as a 'large event', and still represent a major geomorphic response to a severe fire.

Individual charcoal fragments were AMS ^{14}C-dated, using seeds, needles and twigs when available to reduce the probability of dating a sample much older than the fire in which it burned (yielding a large 'inbuilt age'). We obtained 133 dates from 33 stratigraphic sections (sites) in 32 different fans, with 1–15 dates per site (Supplementary Table 1). Calibrated probability distributions[18] for 91 fire-related sedimentation events were summed to produce a probability spectrum (Fig. 2); multiple dates for the same fire-related event and stratigraphically inverted ages (Supplementary Table 2) were excluded. Small events dominate the overall record and are primarily responsible for major peaks except at ~750–1,000 and 1,700 calibrated calendar years before present (cal. yr BP). At-a-site frequency values were calculated to represent the frequency of fire-related events in a single fan's basin. Deposits of single events usually cover only part of a fan, and low- to moderate-severity fires often result in little or no deposits, thus at-a-site frequency of fire-related sedimentation is much lower than

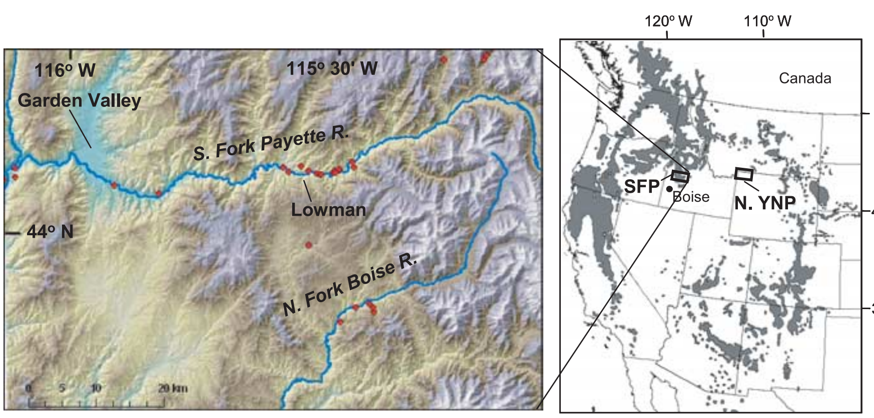

Figure 1 The SFP and northern Yellowstone National Park (YNP) field areas. Right, grey shading shows distribution of *Pinus ponderosa* (ponderosa pine) in the western USA and Canada (ponderosa pine distribution available at http://climchange.cr.usgs.gov/data/atlas). Left, red dots on shaded relief map of the SFP study area show locations of alluvial fan stratigraphic sites. Elevations range from ~850 m in Garden Valley to >2,000 m on the eastern border of the map.

fire frequency in the associated basin. Nonetheless, at-a-site recurrence intervals for small sedimentation events are as low as 33–80 yr. Maxima in small events (Fig. 2a) at ~350, 1,200–1,500, 2,800–3,000, ~5,000 and 6,800–7,400 cal. yr BP correspond with peak at-a-site frequency over the study area, indicating periods of frequent low- to mixed-severity fires that produce limited sedimentation.

In contrast, about 24–27% of the total dated fan thickness was emplaced by only 9 large fire-induced debris-flow events ~1,000–800 cal. yr BP (Fig. 3). The importance of infrequent large events is supported by Holocene-average sediment flux estimates for Idaho batholith basins an order of magnitude greater than modern rates measured without major debris-flow events[11]. Most fans in the lower-elevation ponderosa pine environment contain debris-flow units interbedded with multiple thin sheetflood deposits. Thick (0.5–2 m) fire-related debris-flow deposits dominate higher-elevation fans, consistent with a greater importance of severe stand-replacing fires in mixed-conifer forests.

We compare SFP fire-related sedimentation with a similar record from high-elevation forests in northern Yellowstone National Park (Fig. 1), a cooler and wetter environment than the SFP area, where dense lodgepole-pine-dominated forests burn primarily in large, severe fires with recurrence intervals of 150–400 yr (refs 12, 14, 19). Notably, maxima in small-event probability (Fig. 2a) in the SFP area generally correspond with prominent minima in fire-related sedimentation in Yellowstone (~350–500, 1,200–1,400 and 2,800–3,000 cal. yr BP), suggesting a regional millennial-scale climatic control. In Yellowstone, these minima in fire-related sedimentation are associated with colder, effectively wetter, climates and increased runoff in streams, including during the Little Ice Age (LIA)[12]. LIA climate was not uniformly cold in either time or space, but glacial advances occurred at ~650–100 cal. yr BP in the northern Rocky Mountains[6–8], with colder than present conditions in many Northern Hemisphere localities[8–10].

We infer that over much of the LIA, colder conditions maintained high canopy moisture, inhibiting stand-replacing fires in both Yellowstone lodgepole pine forests and SFP ponderosa pine forests[12–14]. Concurrently, effectively wetter conditions increased understory grass growth and provided fuel for low-severity burns[13] in the SFP, where summers are warmer and drier than in Yellowstone. In ponderosa pine forests, non-lethal surface fires typically occur when several cool, moist years produce abundant fine fuels, followed shortly by a mild to moderate drought year[13,20–22]. Without prolonged severe droughts, wet–dry cycles on annual to multiyear timescales promote frequent fires in the SFP, and an increase in storm frequency during wetter intervals would also augment the number of small fire-related sedimentation events recorded in alluvial fans.

In contrast, intervals of stand-replacing fires and large debris-flow events are largely coincident in SFP ponderosa pine forests and Yellowstone, most notably during the 'Medieval Climatic Anomaly' (MCA), ~1,050–650 cal. yr BP (ref. 23; Fig. 2b). Although often called the 'Medieval Warm Period', times of anomalous Northern Hemisphere warmth are confined to shorter intervals within this period[10,23–25]. In the western USA, the MCA included widespread, severe multidecadal droughts[23,26], with increased fire activity across diverse northwestern conifer forests[12,13]. Some unusually

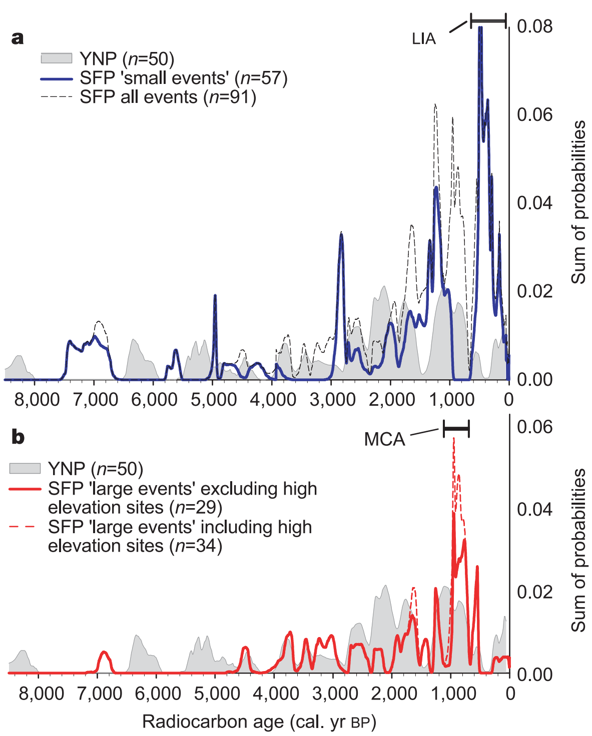

Figure 2 Summed calibrated probability distributions for radiocarbon ages on fire-related sedimentation events in the SFP Idaho area (this study) and in Yellowstone National Park[12] (YNP, grey-filled curves). Probability distributions were smoothed using a 100-yr running mean to reduce the influence of short-period variations in atmospheric ^{14}C, but retain major probability peaks representing the most probable age ranges. Calibrated years before present (cal. yr BP) are equal to the number of calendar years before AD 1950. The general trend of decreasing probability over time, and overall lower probability values before ~4,000 cal. yr BP reflect lesser exposure and preservation of older deposits. **a**, SFP 'small events' (blue line) in Idaho are thin deposits probably related to low- or moderate-severity burns; note correspondence of peaks with minima in YNP fire-related sedimentation, and major peak during the 'Little Ice Age' (LIA), ~650–50 cal. yr BP. (Fewer near-surface deposits in the 400 cal. yr BP–present range were selected for dating because of bioturbation and large uncertainties in ^{14}C calibration.) **b**, SFP 'large events' are major debris-flow deposits probably related to severe fires; note correlation with the YNP record, and prominent peak in large-event probability during the 'Medieval Climatic Anomaly' (MCA), ~1,050–650 cal. yr BP.

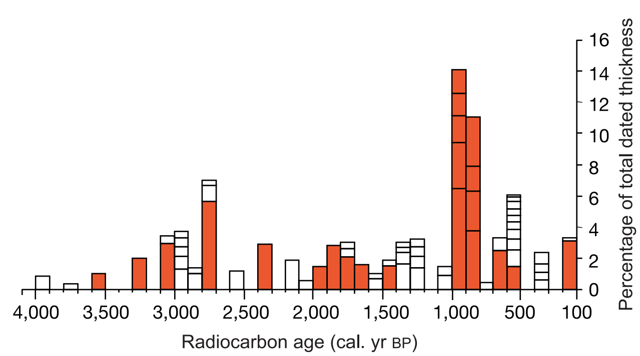

Figure 3 Variations in the thickness of fire-related deposits over time. Relative stratigraphic thickness of dated fire-related fan deposits in the SFP are expressed as a percentage of the total thickness for all dated deposits and plotted by calibrated age interval. Individual deposit thicknesses are shown by stacked bar segments and are calculated as the average of maximum and minimum possible thickness. This range in thickness results from measured variations in deposit thickness and from uncertainty in defining deposit boundaries. Average range of uncertainty in deposit thickness is ±10%. Red bar segments represent 'large events' based on criteria described in the text. Because of calibration problems for very young radiocarbon samples, deposits <100 cal. yr BP are not shown, and data older than 4,000 cal. yr BP are too sparse to be informative. Across the study area, ~50% of the total measured thickness of fan sediments deposited over the past 2,000 yr is probably or possibly related to fire.

wet decades also occurred, at least locally[27]. Despite high fire frequency in the LIA, large SFP debris-flow events during the MCA account for most of the dated fire-related sediment produced over the last millennium (Fig. 3).

Although climate-induced changes in forest composition could drive changes in fire regimes, identification of carbonized macrofossils in fan deposits indicates that at least after ~4,500 cal. yr BP, the same conifer species comprising present forests existed in tributary basins (Supplementary Table 1; Supplementary Fig. 2). The inferred changes in fire frequency and severity may have stemmed in part from changes in relative species abundance—for example, infilling of open ponderosa pine stands by Douglas-fir as in recent decades in central Idaho[3]—but we cannot resolve such spatial changes in forest composition. At site LO1, now characterized by ponderosa pine and minor Douglas-fir, only Douglas-fir was identified at 7,400–6,800 cal. yr BP. Nonetheless, frequent small sedimentation events during this interval suggest a low- to mixed-severity fire regime, similar to ponderosa-dominated stands in the 1600s–1800s (ref. 3).

Along with previous studies covering shorter timescales, our results illustrate how superposed centennial- to millennial-scale climate variations influence fuel conditions, wildfire, and fire-related erosional events. Within multi-centennial cool-moist periods such as the LIA, moderate annual to multi-annual droughts produced frequent fires in xeric SFP ponderosa pine forests, controlled primarily by growth and desiccation of grass and other fine surface fuels. Concurrently, a cooler and effectively moister regional climate inhibited most fires in the high-elevation forests of Yellowstone.

In contrast, extreme droughts of up to multi-decadal length were associated with severe stand-replacing fires and large fire-related erosional events in both the SFP and Yellowstone during the ~400-yr MCA. Denser stands possibly aided these severe fires; perhaps prolonged droughts limited grass growth and surface fires, allowing survival of understory trees as ladder fuels[1–3,13]. Alternatively, decades of unusually wet summers allowed densities to increase. In any case, extreme drought promotes critically low canopy moisture[13] and is associated with MCA stand-replacing fires, despite the absence of fire suppression or land-use effects. Relatively severe droughts within the LIA may have resulted in some stand-replacing fires, as suggested by tree-ring studies in other ponderosa pine forests[22,28,29]. Peak SFP fire-related sedimentation at ~350 cal. yr BP (~AD 1600) may partly reflect a prolonged drought in the late AD 1500s[26]. Nonetheless, limited geomorphic response indicates that fires in the LIA were overall less severe than in either the MCA or recent decades.

Instrumental and proxy records reveal a rapid rise in Northern Hemisphere temperatures over the last century[5,8,9] that is probably in part anthropogenic[24], and current warmth is probably greater than in the MCA[25]. Warming of 0.6–2 °C has affected much of the western USA during the last century, and has been accompanied by a 5–20% decrease in precipitation[30] in northern ponderosa pine environments. Fire-season Palmer drought severity index correlates strongly with burn area in both central Idaho and Yellowstone[12,20], and shows a significant ($P = 0.01$) increase in drought severity between 1895 and 2002. In addition, twentieth-century fire suppression and to a lesser extent grazing have limited surface fires, allowing seedling survival and increased densities in SFP ponderosa pine stands[3]. Alteration of fuel conditions combined with increased incidence of extreme drought have probably produced the recent spate of extensive severe fires in the SFP and other northern ponderosa pine forests.

Fire management and ecological restoration strategies in ponderosa pine forests typically aim to prevent large stand-replacing fires by reproducing pre-settlement conditions with low tree densities[1,3]. Climate exerts a powerful control on fire regimes, however, and the rapidity and magnitude of twentieth-century global climate change is probably greater than has occurred for millennia[24,25]. Efforts to return to fire regimes typical of a generally colder pre-settlement era will need to adapt to changing vegetation and fire activity in a warmer and drought-prone future. □

Received 17 February; accepted 15 September 2004; doi:10.1038/nature03058.

1. Covington, W. W. *et al.* Historical and anticipated changes in forest ecosystems of the inland west of the United States. *J. Sustain. For.* **2,** 13–63 (1994).
2. Agee, J. K. *Fire Ecology of Pacific Northwest Forests* (Island, Washington DC, 1993).
3. Steele, R., Arno, S. F. & Geier-Hayes, K. Wildfire patterns change in central Idaho's ponderosa pine-Douglas-fir forest. *West. J. Appl. For.* **1,** 16–18 (1986).
4. Meyer, G. A., Pierce, J. L., Wood, S. H. & Jull, A. J. T. Fires, storms, and erosional events in the Idaho batholith. *Hydrol. Process.* **15,** 3025–3038 (2001).
5. Mann, M. E., Bradley, R. S. & Hughes, M. K. Northern hemisphere temperatures during the past millennium: inferences, uncertainties, and limitations. *Geophys. Res. Lett.* **26,** 759–762 (1999).
6. Carrara, P. E. Late Quaternary glacial and vegetative history of the Glacier National Park region, Montana. *US Geol. Surv. Bull.* **1902,** 1–64 (1989).
7. Luckman, B. H. The Little Ice Age in the Canadian Rockies. *Geomorphology* **32,** 357–394 (2000).
8. Grove, J. M. *The Little Ice Age* (Methuen, New York, 1988).
9. Pollack, H. N., Huang, S. & Shen, P. Climate change record in subsurface temperatures: a global perspective. *Science* **282,** 279–281 (1998).
10. Esper, J., Cook, E. R. & Schweingruber, F. H. Low-frequency signals in long tree-ring chronologies for reconstructing past temperature variability. *Science* **295,** 2250–2253 (2002).
11. Kirchner, J. W. *et al.* Mountain erosion over 10 yr, 10 k.y., and 10 m.y. time scales. *Geology* **29,** 591–594 (2001).
12. Meyer, G. A., Wells, S. G. & Jull, A. J. T. Fire and alluvial chronology in Yellowstone National Park: Climatic and intrinsic controls on Holocene geomorphic processes. *Geol. Soc. Am. Bull.* **107,** 1211–1230 (1995).
13. Rollins, M. G., Morgan, P. & Swetnam, T. Landscape-scale controls over 20th century fire occurrence in two large Rocky Mountain (USA) wilderness areas. *Landscape Ecol.* **17,** 539–557 (2002).
14. Whitlock, C., Shafer, S. L. & Marlon, J. The role of climate and vegetation change in shaping past and future fire regimes in the northwestern US and the implications for ecosystem management. *For. Ecol. Manage.* **178,** 163–181 (2003).
15. Moody, J. A. & Martin, D. A. Comparison of soil infiltration rates in burned and unburned mountainous watersheds. *Hydrol. Process.* **15,** 2981–2993 (2001).
16. Lavee, H., Kutiel, P., Segev, M. & Benyamini, Y. Effect of surface roughness on runoff and erosion in a Mediterranean ecosystem: the role of fire. *Geomorphology* **11,** 227–234 (1995).
17. Schmidt, K. M. *et al.* The variability of root cohesion as an influence on shallow landslide susceptibility in the Oregon Coast Range. *Can. Geotech. J.* **38,** 995–1024 (2001).
18. Stuiver, M. & Reimer, P. J. Extended ^{14}C data base and revised CALIB 3.0 ^{14}C age calibration program. *Radiocarbon* **35,** 215–230 (1993).
19. Barrett, S. W. Fire regimes on andesitic mountain terrain in northeastern Yellowstone National Park, Wyoming. *Int. J. Wildl. Fire* **4,** 65–76 (1994).
20. Westerling, A. L., Gershunov, A., Brown, T. J., Cayan, D. R. & Dettinger, M. D. Climate and wildfire in the western United States. *Bull. Am. Meteorol. Soc.* **84,** 595–604 (2003).
21. Swetnam, T. W. & Betancourt, J. L. Mesoscale disturbance and ecological response to decadal climatic variability in the American Southwest. *J. Clim.* **11,** 3128–3147 (1998).
22. Veblen, T. T., Kitzberger, T. & Donnegan, J. Climatic and human influences on fire regimes in ponderosa pine forests in the Colorado Front Range. *Ecol. Appl.* **10,** 1178–1195 (2000).
23. Stine, S. in *Water, Environment and Society in Times of Climatic Change* (eds Issar, A. S. & Brown, N.) 43–67 (Kluwer, Dordrecht, 1998).
24. Crowley, T. J. Causes of climate change over the past 1000 years. *Science* **289,** 270–277 (2000).
25. Bradley, R. S., Hughes, M. K. & Diaz, H. F. Climate in medieval time. *Science* **302,** 404–405 (2003).
26. Woodhouse, C. A. & Overpeck, J. T. 2000 years of drought variability in the central United States. *Bull. Am. Meteorol. Soc.* **79,** 2693–2714 (1998).
27. Adams, K. Age and paleoclimatic significance of late Holocene lakes in the Carson Sink, NV, USA. *Quat. Res.* **60,** 294–305 (2003).
28. Brown, P. M., Kaufmann, M. R. & Shepperd, W. D. Long-term, landscape patterns of past fire events in a montane ponderosa pine forest of central Colorado. *Landscape Ecol.* **14,** 513–532 (1999).
29. Shinneman, D. J. & Baker, W. L. Nonequilibrium dynamics between catastrophic disturbances and old-growth forests in ponderosa pine landscapes of the Black Hills. *Conserv. Biol.* **11,** 1276–1288 (1997).
30. Karl, T. R., Knight, R. W., Easterling, D. R. & Quayle, R. G. Indices of climate change for the United States. *Bull. Am. Meteorol. Soc.* **77,** 279–286 (1996).

Supplementary Information accompanies the paper on **www.nature.com/nature**.

Acknowledgements Research funding was provided by the NSF, the University of New Mexico (UNM) and the UNM Department of Earth and Planetary Sciences. We thank L. Huckell for assistance with macrofossil identification; K. Pierce, B. Huckell and L. McFadden for comments on the manuscript; and S. Wood, T. Lite, L. Rockwell, S. Caldwell, C. North, K. Grover-Wier, K. Pierce and W. Andersen for discussions and field assistance.

Competing interests statement The authors declare that they have no competing financial interests.

Correspondence and requests for materials should be addressed to J.P. (jpierce@unm.edu).